

Full Paper

Synthesis, Anti-Inflammatory Activity, and COX-1/2 Inhibition Profile of Some Novel Non-Acidic Polysubstituted Pyrazoles and Pyrano[2,3-*c*]pyrazoles

Hassan M. Faidallah¹ and Sherif A. F. Rostom ^{2,3}

¹ Department of Chemistry, Faculty of Science, King Abdulaziz University, Jeddah, Saudi Arabia

² Department of Pharmaceutical Chemistry, Faculty of Pharmacy, King Abdulaziz University, Jeddah, Saudi Arabia

³ Department of Pharmaceutical Chemistry, Faculty of Pharmacy, University of Alexandria, Alexandria, Egypt

The synthesis and evaluation of the anti-inflammatory activity of some structure hybrids comprising basically the 5-hydroxy-3-methyl-1-phenyl-4-substituted-1*H*-pyrazole scaffold directly linked to a variety of heterocycles and functionalities, or annulated as pyrano[2,3-*c*]pyrazoles, is described. According to the *in vivo* results and a comprehensive structure–activity relationship study, five analogs (**5**, **10**, **17**, **19**, and **27**) displayed remarkable anti-inflammatory profiles showing distinctive % protection and ED₅₀ values, especially **10** and **27** (ED₅₀ 35.7 and 38.7 μmol/kg, respectively) which were nearly equiactive to celecoxib (ED₅₀ 32.1 μmol/kg). Compounds **10**, **17**, and **27** exhibited distinctive COX-2 inhibition with a noticeable COX-2 selectivity (SI values 7.83, 6.87, and 7.16, respectively), close to that of celecoxib (SI 8.68). Additionally, **5**, **10**, **17**, **19**, and **27** proved to be gastrointestinal tract safe (0–20% ulceration) and non-toxic, being well tolerated by the experimental animals up to 250 mg/kg orally and 80 mg/kg parenterally. Collectively, the *in vivo* ED₅₀ values for the most potent five derivatives agree with their *in vitro* COX-2 selectivity indices, suggesting their usefulness as selective anti-inflammatory COX-2 inhibitors. The bipyrazole **10** and the pyranopyrazole **27** could be considered as the most active members in this study, being nearly equiactive to celecoxib, besides their obvious selective COX-2 inhibition, high safety margin, and predicted pharmacokinetic (ADME-T) suitability for oral use.

Keywords: Anti-inflammatory activity / COX-1 / COX-2 / Pyrazole / Selective COX-2 inhibitors

Received: January 22, 2017; Revised: March 1, 2017; Accepted: March 7, 2017

DOI 10.1002/ardp.201700025



Additional supporting information may be found in the online version of this article at the publisher's web-site.

Introduction

The phenomenon of “inflammation” signalizes a reaction to any mechanical damage or infection facing the human body. Subsequently, cases, such as chronic infections, degenerative

processes (as in osteoarthritis), or different autoimmune diseases, might be referred to as “inflammatory conditions” [1]. Non-steroidal anti-inflammatory drugs (NSAIDs) constitute one of the most public classes of drugs that are utilized for alleviation of pain and inflammatory conditions connected with various pathophysiological conditions. Their pharmacological action relies on the interference in the biosynthesis of prostaglandins (PGs) through inhibition of the cyclooxygenase (COX) enzyme [2]. PGs are known to be implemented in the induction of inflammation, some homeostatic processes as well as cytoprotection of the gastrointestinal tract (GIT). Therefore, extensive and

Correspondence: Prof. Sherif A. F. Rostom, Department of Pharmaceutical Chemistry, Faculty of Pharmacy, King Abdulaziz University, PO Box 80260, Jeddah 21589, Saudi Arabia.

E-mail: sherifrostom@yahoo.com

Fax: +9662-6400000-22327

inappropriate administration of NSAIDs mostly leads to GI problems (e.g., induction of gastric ulcer), blood, kidney, and liver serious harmful effects [3]. A new era in the anti-inflammatory research area has been entered when it has been assessed that COX is available as two isozymes, COX-1 and COX-2, which are controlled with different conditions [4]. COX-1 is naturally occurring and is concerned with the production of the protective PGs in the GI and thromboxanes in blood platelets [5]. In contrast, COX-2 is an inducible isozyme and is stimulated as a result of the release of inflammatory mediators during the inflammation process [6]. Subsequently, the peculiar distribution of the two isozymes among different tissues has provoked the search for novel NSAIDs with distinctive therapeutic activity based on selective inhibition of COX-2 that would stop the production of the inflammatory PGs, while sparing GI-protective effects regulated by COX-1 [7]. As a result, many selective inhibitors of COX-2 (coxibs) have been introduced to the market with variable anti-inflammatory potentials and safety margins. Unfortunately, prolonged use of some coxibs (e.g., rofecoxib and valdecoxib) resulted in serious cardiovascular disorders [8], which determined the dragging of these coxibs [9] and clearly urged the need to find out new scaffolds having COX-2 inhibitory activity.

Among the family of biologically active heterocycles, special interest has been given to pyrazole-containing compounds as potential anti-inflammatory, antinociceptive, and antipyretic agents [10–17] especially after the discovery of antipyrine at 1884 as the first anti-inflammatory pyrazole analog. As a consequence, a tremendous number of pyrazoles has been prepared, biologically investigated, and some of them have been introduced clinically. As a prominent example, the currently available selective COX-2 inhibitor

celecoxib (Fig. 1) is a pyrazole derivative with distinctive anti-inflammatory and GI safe effects [18]. During our continuous search for novel pyrazole candidates endowed with potential bioactivities [19–33], we have reported on the synthesis, *in vivo* and *in vitro* anti-inflammatory activities of some lead structures comprising mainly the 1-arylpyrazol(in)e counterpart substituted with several functionalities and/or attached to different heterocyclic rings through various linkages [27–33]. In particular, potential anti-inflammatory activity was ascribed to the pyrazolyl compounds **A** [30], **B** [31], and **C** [32] (Fig. 1) and the bipyrazolyl derivatives **D** [33] (Fig. 1).

Inspired by these facts, the objective of this research is to develop and investigate the *in vivo* as well as *in vitro* anti-inflammatory potentials of some novel non-acidic polyfunctional pyrazoles. The targeted compounds were rationalized so as to comprise basically the 5-hydroxy-3-methyl-1-phenyl-4-substituted-1*H*-pyrazole scaffold substituted at position-4 with a variety of heterocycles known for their relevant biological activities including the isoxazole, pyrazole, pyrimidine, tetrazolo[1,5-*a*]pyrimidine, triazolo[4,3-*a*]pyrimidine, and pyrimido[2,1-*c*][1,2,4]triazine ring systems (**E**; Fig. 1). This combination was suggested in an attempt to investigate the influence of such hybridization and structure variation on the anticipated anti-inflammatory potential and safety profile, hoping to add some biological synergism to the target molecules. Moreover, the substitution pattern of the target compounds was aimed to include some pharmacophores that are believed to be highly contributing to the anticipated biological activity such as the sulfonamide, azomethine, sulfonylureido, and sulfonylthioureido functionalities. Furthermore, annulation of the main pyrazole ring into the corresponding substituted pyrano[2,3-*c*]pyrazoles (**F**; Fig. 1) was thought to be an interesting structure variation through

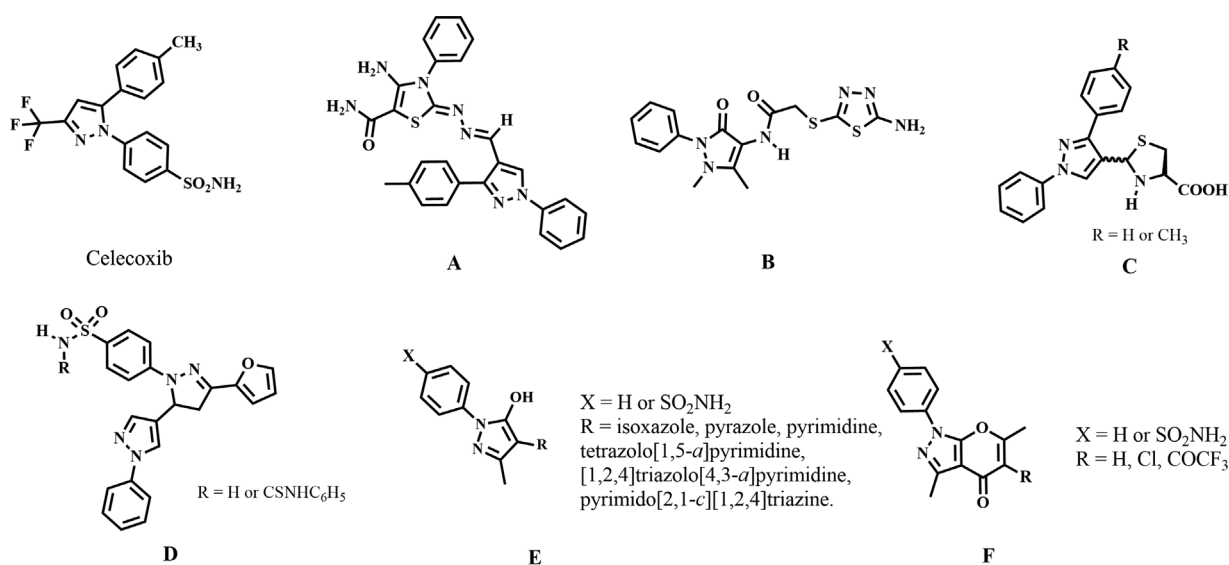


Figure 1. Structures of celecoxib, the lead compounds **A–D**, and the general formulae of the novel series of compounds **E** and **F**.

affecting the electronic and/or steric environment of the molecules that might have an impact on the targeted biological activity. It should be noted that, in addition to the targeted anti-inflammatory activity, the ulcerogenic and acute toxicity profiles of the active compounds were also evaluated. Besides, an *in silico* computation of the molecular properties, physicochemical profile, drug score, and drug-likeness of the biologically active compounds was performed to predict their pharmacokinetic and toxicity properties (ADME-T), and to assess their suitability as possible orally active drug candidates.

Results and discussion

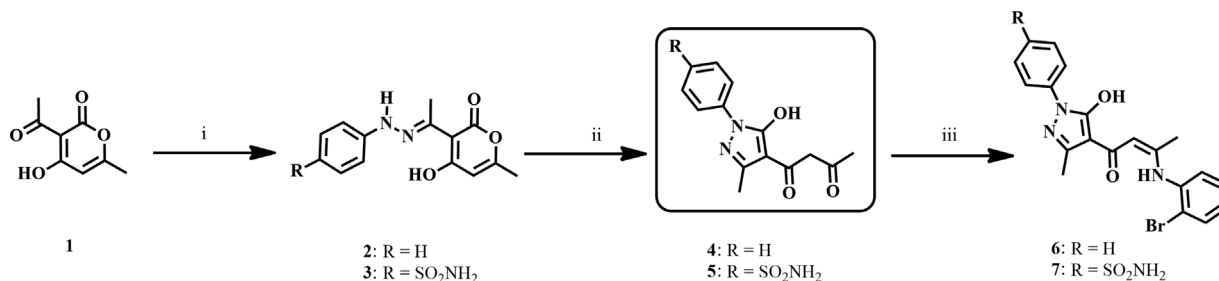
Chemistry

The synthetic strategies employed to obtain the intermediate and target compounds are illustrated in Schemes 1–4. In Scheme 1, condensation of the precursor dehydroacetic acid (DHA) with the appropriate arylhydrazine afforded the corresponding arylhydrazones **2** and **3**. Heating these arylhydrazones with acetic acid gave rise to the corresponding substituted 1-(5-hydroxy-3-methyl-1-phenyl-1*H*-pyrazol-4-yl)butane-1,3-diones **4** and **5**, which were employed as the principle key intermediates in this study. Their IR spectra were characterized by the appearance of two carbonyl absorption bands at 1622–1635 cm^{-1} and 1715–1724 cm^{-1} , respectively, as well as an exchangeable OH band at 3328–3398 cm^{-1} . Reacting the pyrazoles **4** and **5** with 2-bromoaniline yielded the target 2-bromophenylamino derivatives **6** and **7**.

In Scheme 2, condensation of the pyrazole precursors **4** and **5** with hydroxyl amine gave rise to the corresponding 3-methylisoxazol-5-yl derivatives **8** and **9**. Furthermore, cyclocondensation of the pyrazolylbenzenesulfonamide **5** with phenylhydrazine yielded the corresponding bipyrazole **10** which was subjected to different condensation reactions. For instance, condensing **10** with 4-chlorobenzaldehyde in acetic acid afforded the expected azomethine derivative **11**. Meanwhile, nucleophilic addition reaction of the bipyrazole **10** across the N=C bond of the 4-chlorophenyl isocyanate or 4-

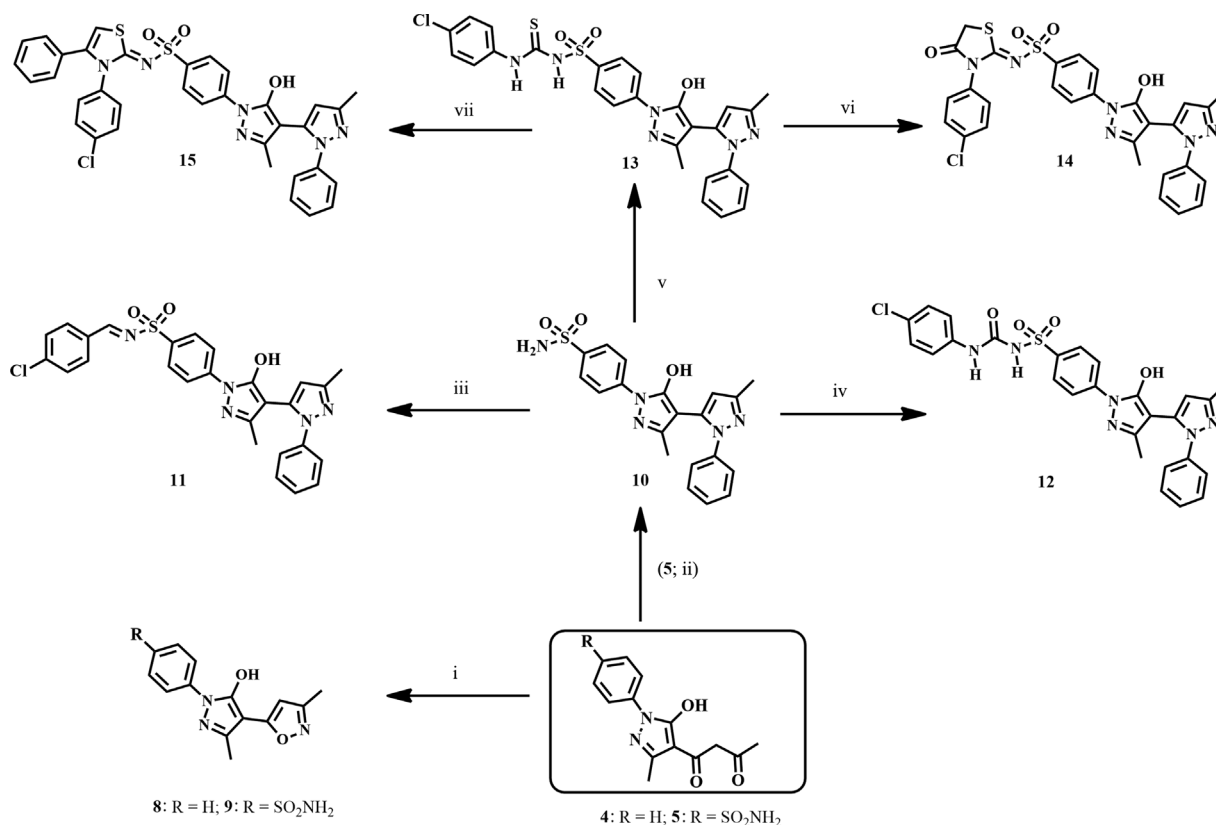
chlorophenyl isothiocyanate and anhydrous K_2CO_3 in dry acetone, afforded the corresponding substituted sulfonylureido and sulfonylthioureido derivatives **12** and **13**, respectively. Their IR spectra exhibited two absorption bands at 1164–1169 cm^{-1} and 1336–1368 cm^{-1} due to the SO_2N group besides a ureido carbonyl band at 1652 cm^{-1} (for **12**) and a thioureido absorption band at 1155 cm^{-1} (for **13**). In its turn, cyclcondensation of the sulfonylthioureido derivative **13** with ethyl bromoacetate or phenacyl bromide in the presence of anhydrous Na acetate produced the corresponding 4-oxothiazolidine **14** and the thiazoline **15**. The IR spectrum of **14** was characterized by the sharp band at 1712 cm^{-1} due to the thiazolidine C_4 carbonyl group, while its ^1H NMR spectrum showed a new singlet at δ 3.42 ppm owing to the thiazolidine C_5 methylene protons. In contrast, the ^1H NMR of the thiazoline **15** exhibited a new singlet at δ 5.63 ppm due to the thiazoline C_5 proton.

As shown in Scheme 3, cyclocondensation of the pyrazolylbutane-1,3-dione **4** with thiourea or methylthiourea produced the corresponding pyrimidine-2-thiones **16** and **17**, respectively. Their IR spectra exhibited characteristic absorption bands at 1182–1192 cm^{-1} , while their ^{13}C NMR exhibited peaks at δ 180.40–185.02 ppm attributed to the thiocarbonyl functionality. Cyclocondensation of the pyrimidinethione **16** with hydrazine hydrate gave the key intermediate 2-hydrazino derivative **18**. In its turn, when a solution **18** in acetic acid was reacted with sodium nitrite at room temperature, the tetrazolo-[1,5-*a*]pyrimidine **19** was obtained. Moreover, refluxing **18** with acetylacetone or ethyl bromoacetate yielded the targeted substituted [1,2,4]triazolo[3,4-*a*]pyrimidines **20** and **21**, respectively, following a reported procedure [34]. Whereas reacting **18** with an excess of diethyl oxalate gave the corresponding ethyl [1,2,4]triazolo[3,4-*a*]pyrimidine-3-carboxylate analog **22**. Here, it should be noted that reaction of **18** with an equivalent amount of diethyl oxalate in the presence of sodium acetate yielded the pyrimido[2,1-*c*][1,2,4]triazine-3,4-dione **23**, where the ^1H -NMR lacked the triplet and quartet protons of the ethoxy group which proved the aminolysis of the ester function. Meanwhile, the IR spectrum of **23** showed two carbonyl absorptions at 1665 and 1678 cm^{-1} . Finally,



Reagents and reaction conditions: (i) 4-R- $\text{C}_6\text{H}_4\text{NHNH}_2$, benzene, reflux, 1 h; (ii) HOAc, reflux, 2–3 h; (iii) aryl amine, EtOH, reflux, 3 h.

Scheme 1. Synthesis of compounds **2–7**.



Reagents and reaction conditions: (i) NH₂OH·HCl, EtOH/HOAc, reflux, 2 h; (ii) **5**, 4-SO₂NH₂-C₆H₄NHNH₂, EtOH, reflux, 3 h; (iii) R-C₆H₄-CHO, HOAc, reflux, 6-8 h; (iv) 4-Cl-C₆H₄-NCO, K₂CO₃, acetone, reflux, 18 h; (v) **31**, 4-Cl-C₆H₄-NCS, K₂CO₃, acetone, reflux, 10 h; (vi) ethyl bromoacetate, Na acetate, EtOH, reflux, 2 h; (vii) phenacyl bromide, Na acetate, EtOH, reflux, 2 h.

Scheme 2. Synthesis of compounds **8–15**.

cyclocondensation of the **18** with β-bromoketones in acetic acid gave rise to the substituted pyrimido[2,1-c][1,2,4]triazines **24** and **25**.

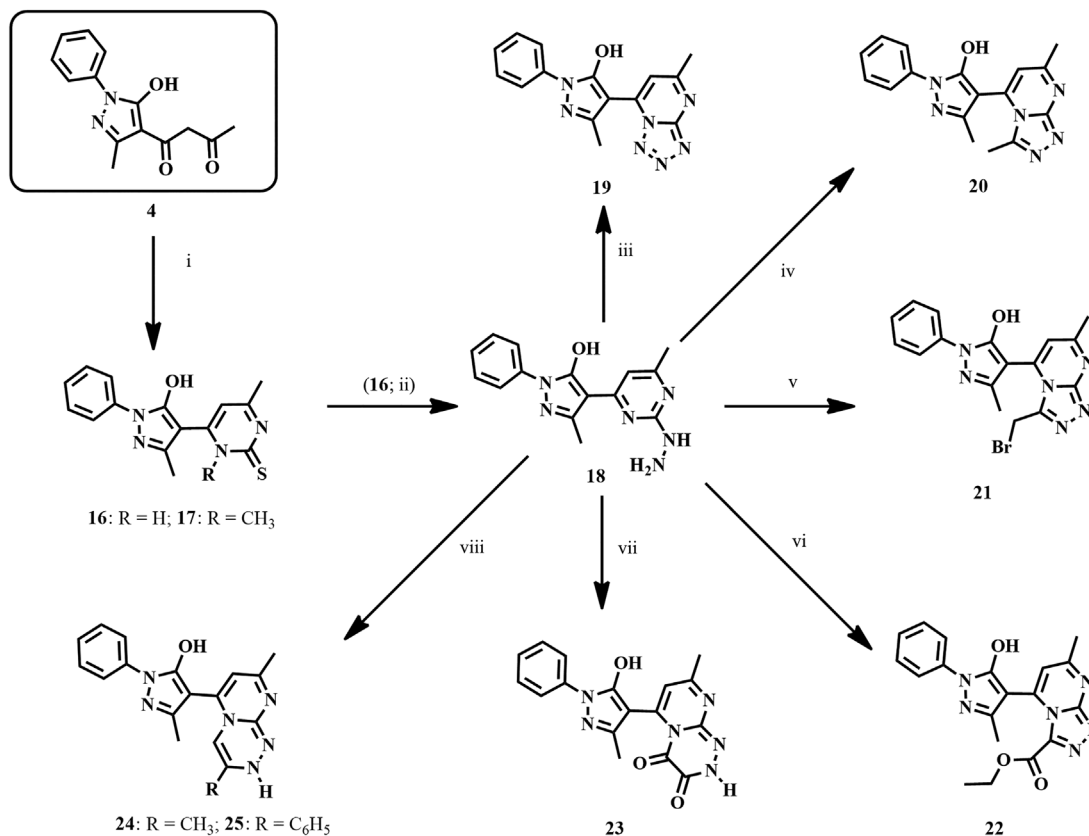
At this stage, it was attempted to annulate the pyrazolylbutane-1,3-diones **4** and **5** into the corresponding pyrano[2,3-c]pyrazoles as illustrated in Scheme 4. In this view, ring closure of **4** and **5** into the 3,6-dimethyl-1-(4-substitutedphenyl)pyrano[2,3-c]pyrazol-4(1H)-ones **26** and **27** was easily accomplished via treatment of their solutions in acetic acid with sulfuric acid at room temperature. Their IR spectra exhibited carbonyl absorption bands at 1660–1664 cm⁻¹, whereas their ¹H NMR showed two methyl singlets at δ 2.04–2.10 and δ 2.44–2.47 ppm. Furthermore, treatment of the starting pyrazoles **4** and **5** with sulfonyl chloride or trifluoroacetic anhydride gave rise to the corresponding 3-chloro **28** or the 3-trifluoroacetyl derivatives **30** and **31**, respectively, which were directly cyclodehydrated (without purification) with concentrated sulfuric acid at room temperature to the corresponding 4-oxo-1H-pyrano[2,3-c]pyrazoles **29**, **32**, and **33**. The IR

spectrum of the 5-chloropyranopyrazole **29** showed a carbonyl absorption at 1665 cm⁻¹, while the analogs **32** and **33** exhibited two carbonyl bands at 1662–1668 cm⁻¹ and 1669–1672 cm⁻¹. The ¹³C NMR data showed a characteristic carbonyl carbon at δ 186.56 ppm for **29**, and two carbonyl signals at δ 183.66–185.23 and δ 196.20–196.60 ppm for **32** and **33**, respectively.

Biological evaluation

Carrageenan-induced paw edema

All the synthesized 27 target compounds (**4–27**, **29**, **32**, and **33**) were evaluated for their *in vivo* systemic anti-inflammatory activity using the carrageenan-induced paw edema bioassay in rats [35] as a model of acute inflammation. Indomethacin and celecoxib were employed as standard anti-inflammatory agents against COX-1 and COX-2 enzymes, respectively. The data obtained are presented in Table 1 as the mean increase in paw edema (mL) ± SE. The results showed that 18 compounds (**4**, **5**, **7**, **9–13**, **16–20**, **24**, **26**, **27**, **29**, and **33**) were able to exhibit variable degree of systemic anti-inflammatory potential.



Reagents and reaction conditions: (i) RNHCSNH₂, EtOH, reflux, 6 h; (ii) NH₂NH₂·98%, EtOH, r.t., 2 h; (iii) gl. HOAc, aq. NaNO₂, r.t., 3 h; (iv) acetyl acetone, EtOH, reflux, 8 h; (v) ethyl bromoacetate, EtOH, reflux, 2 h; (vi) diethyl oxalate (excess), reflux, 3 h; (vii) diethyl oxalate, Na acetate, EtOH, reflux, 8 h; (viii) RCOCH₂Br, gl. HOAc, reflux, 2 h.

Scheme 3. Synthesis of compounds 16–25.

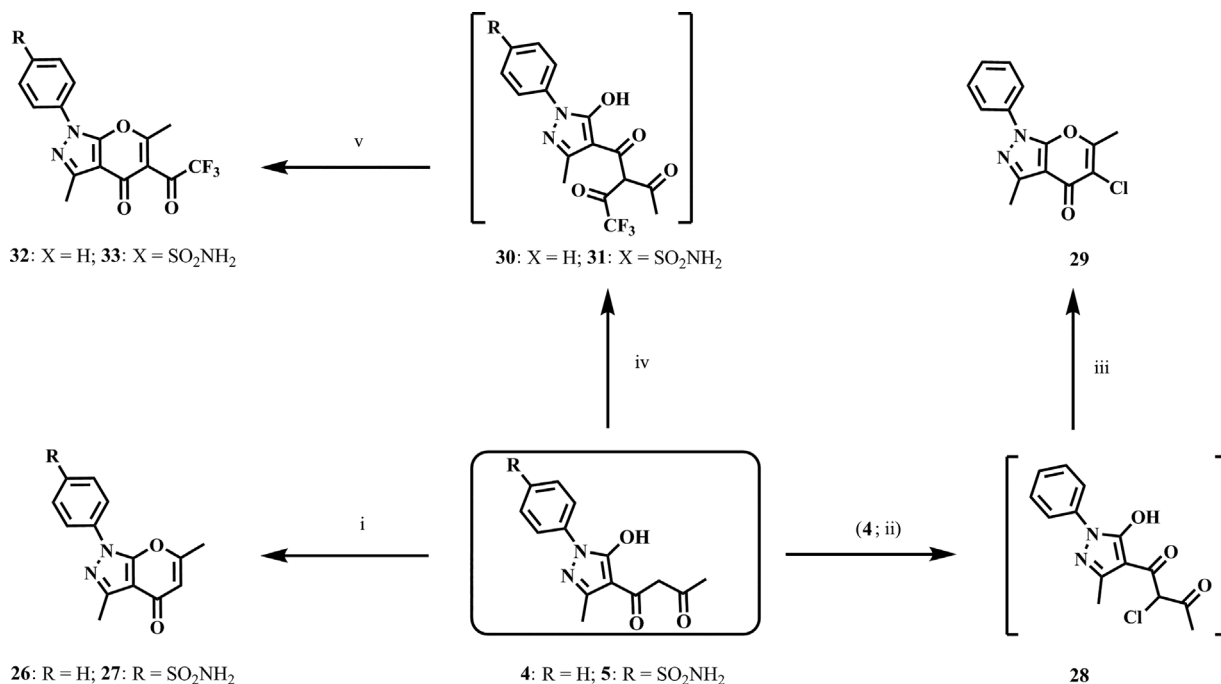
Compounds **5**, **10**, **17**, **19**, and **27** proved to be the most active anti-inflammatory agents in the present study as evidenced from their distinctive % protection values (68.5, 74.2, 69.7, 67.4, and 70.8%, respectively), which are comparable or even better than those of indomethacin and celecoxib (% protection 70.8 and 75.3, respectively) under the same experimental conditions. Meanwhile, the analogs **4**, **16**, **20**, and **24** displayed noticeable anti-inflammatory potentials as seen from their % protection values (60.7–65.2%), constituting 85.7–92.1% of the activity of indomethacin and 80.6–86.6% of that of celecoxib. Moreover, **7**, **9**, **13**, **18**, **26**, and **33** exhibited moderate activity (% protection range 50.6–59.6%) representing 71.5–84.2% of the activity of indomethacin and 67.2–79.2% of that of celecoxib. Whereas, **11**, **12**, and **29** showed weak anti-inflammatory activity (% protection 38.2–49.4%).

For further assessment of the anti-inflammatory potential, the ED₅₀ values of the five prominently active compounds **5**, **10**, **17**, **19**, and **27** were determined [36]. The results presented in Table 1 revealed that all the five tested compounds possess

a considerable anti-inflammatory potential (ED₅₀ values 68.2, 35.7, 53.1, 75.2, and 38.7 μmol/kg, respectively), when compared with celecoxib (ED₅₀ 32.1 μmol/kg). In particular, the bipyrazole **10** and pyranopyrazole **27** (ED₅₀ 35.7 and 38.7 μmol/kg, respectively) stemmed as the most potent members being nearly equiactive to celecoxib (ED₅₀ 32.1 μmol/kg). The remaining three analogs showed moderate anti-inflammatory potency with ED₅₀ values ranging between 53.1 and 75.2 μmol/kg.

Structure–activity correlation

A close examination of the structures of the active compounds in relation to their % protection capabilities revealed that the anti-inflammatory activity was greatly affected by the type of substituent at C₄ of the main pyrazole scaffold. For instance, better anti-inflammatory activity was often linked with analogs comprising the pyrazolyl, pyrimidinyl, tetrazolopyrimidinyl counterparts, in addition to the pyrano[2,3-c]-pyrazole structure variant. In this view, in Scheme 1, among



Reagents and reaction conditions: (i) HOAc, H₂SO₄, r.t., 2 h; (ii) SO₂Cl₂, CH₂Cl₂, r.t., 2 h; (iii) C, H₂SO₄, r.t., 4 h; (iv) (CF₃CO)₂O, THF, reflux, 4 h; (v) C, H₂SO₄, r.t., 4 h

Scheme 4. Synthesis of compounds 26–33.

the parent 1-(5-hydroxy-3-methyl-1-(4-substituted phenyl)-1*H*-pyrazol-4-yl)butane-1,3-diones **4** and **5**, compound **5** (R = SO₂NH₂) showed remarkable anti-inflammatory activity (% protection 68.5) comparable with indomethacin and celecoxib (70.8 and 75.3%, respectively). Introduction of a (2-bromophenyl)amino counterpart as in **7** (R = SO₂NH₂) resulted in a marked reduction in the activity (% protection 50.6). Similarly, incorporation of the butane-1,3-dione moiety of the parent pyrazoles **4** and **5** into an isoxazole ring (**9**; R = SO₂NH₂) led to an obvious decrease in the activity (Scheme 2). On the other hand, a significant improvement in the anti-inflammatory potential was obtained via cyclization of the pyrazole **5** into the corresponding bipyrazole structure **10** which was stemmed as the most active member in this study (% protection 74.2), being more potent *in vivo* than indomethacin and nearly equiactive to celecoxib. Here, it is worth mentioning that the substitution pattern of the bipyrazole **10** is structurally relevant to the vicinal diaryl heterocycles template of COX-2 inhibitors represented by celecoxib, in which the benzenesulfonamide moiety was replaced with a sulfonamide-substituted arylpyrazole counterpart (Fig. 2). However, further derivatization of the sulfonamido group of **10** into the substituted benzylidene **11**, sulfonylureido **12**, and sulfonylthioureido **13** functionalities

led to a noticeable lowering of the anti-inflammatory potential. Subsequent rigidification of the sulfonylthioureido group into either thiazolidinedione **14** or thiazolines **15** ring systems led to complete abolishment of activity. Such dramatic collapse in the bioactivity of the analogs **11–15** could be attributed to their steric bulkiness which would probably affect bioavailability and/or binding with COX enzymes. Variation of the substituent type at C₄ of the main pyrazole scaffold **4** was extended to produce the substituted pyrazolopyrimidines **16** and **17** which showed acceptable anti-inflammatory capability, especially **17** (R = SO₂NH₂) with % protection of 69.7 (Scheme 3). Conversion of the thione into the hydrazine function as in **18** led to a clear drop in the activity, presumably due to increasing compound's polarity. Further cyclization of **18** into the corresponding tetrazolo[1,5-*a*]pyrimidine **19** has obviously improved the activity probably due to the presence of multiple H-bond forming centers that would assist binding with the COX enzymes. However, bioisosteric replacement of the tetrazolo[1,5-*a*]pyrimidine moiety with substituted 1,2,4-triazolo[4,3-*a*]pyrimidine counterparts **20–22** furnished only one active compound **20** with less anti-inflammatory potential. Whereas, increasing ring size by incorporating the pyrimidine ring of **18** into a pyrimido[2,1-*c*][1,2,4]triazine ring system yielded three compounds **23–25** among which the analog **24** was the only

Table 1. *In vivo* anti-inflammatory activity (carrageenan-induced rat paw edema bioassay) and the ulcerogenic effect of the active compounds.

Compound number	Increase in paw edema (mL) ^{a)}	Protection (%)	AI % relative to indom. ^{b)}	AI % relative to celecoxib ^{c)}	ED ₅₀ (μmol/kg)	Ulceration ^{d)} (%)
Control	0.89 ± 0.025	0.0	0.0	0.0	–	–
Indomethacin ^{b)}	0.26 ± 0.021	70.8	100	94	ND ^{e)}	100
Celecoxib ^{c)}	0.22 ± 0.015	75.3	106.4	100	32.1	40
4	0.35 ± 0.021	60.7	85.7	80.6	ND	ND
5	0.28 ± 0.015	68.5	96.8	91.0	68.2	20
7	0.44 ± 0.019	50.6	71.5	67.2	ND	ND
9	0.41 ± 0.025	53.9	76.1	71.5	ND	ND
10	0.23 ± 0.015	74.2	104.8	98.5	35.7	20
11	0.49 ± 0.023	44.9	63.4	59.6	ND	ND
12	0.55 ± 0.011	38.2	53.9	50.7	ND	ND
13	0.38 ± 0.017	57.3	80.9	76.1	ND	ND
16	0.31 ± 0.024	65.2	92.1	86.6	ND	ND
17	0.27 ± 0.018	69.7	98.4	92.6	53.1	0.0
18	0.36 ± 0.023	59.6	84.2	79.2	ND	ND
19	0.29 ± 0.018	67.4	95.2	89.5	75.2	0.0
20	0.32 ± 0.023	64.0	90.4	85.0	ND	ND
24	0.34 ± 0.021	61.2	86.4	81.3	ND	ND
26	0.37 ± 0.015	58.4	82.5	77.6	ND	ND
27	0.26 ± 0.014	70.8	100	94.1	38.7	0.0
29	0.45 ± 0.012	49.4	69.8	65.6	ND	ND
33	0.42 ± 0.023	52.8	74.6	70.1	ND	ND

^{a)} Values were determined after 4 h and are expressed as mean (mL) ± SE (no. of animals per experimental group *N* = 5). All data are significantly different from control (*P* < 0.05).

^{b,c)} AI%: percentage anti-inflammatory activity relative to indomethacin and celecoxib; reference standard COX-1 and COX-2 inhibitors, respectively.

^{d)} Five animals per experimental group.

^{e)} ND: not determined.

active analog with moderate bioactivity. On the other hand, annulation of the parent pyrazolyl butane-1,3-diones **4** and **5** into the corresponding bicyclic substituted 3,6-dimethyl-1-phenylpyrano[2,3-*c*]pyrazole-4(1*H*)-ones (Scheme 4) furnished four active compounds (**26**, **27**, **29**, and **33**), which carry some

structure relevance to the vicinal diaryl heterocycles template of COX-2 inhibitors represented by celecoxib (Fig. 2). The anti-inflammatory profile of these derivatives was modulated by the type of substituent at position 5. For instance, the sulfonamido derivative **27** (R = SO₂NH₂) revealed remarkably improved anti-

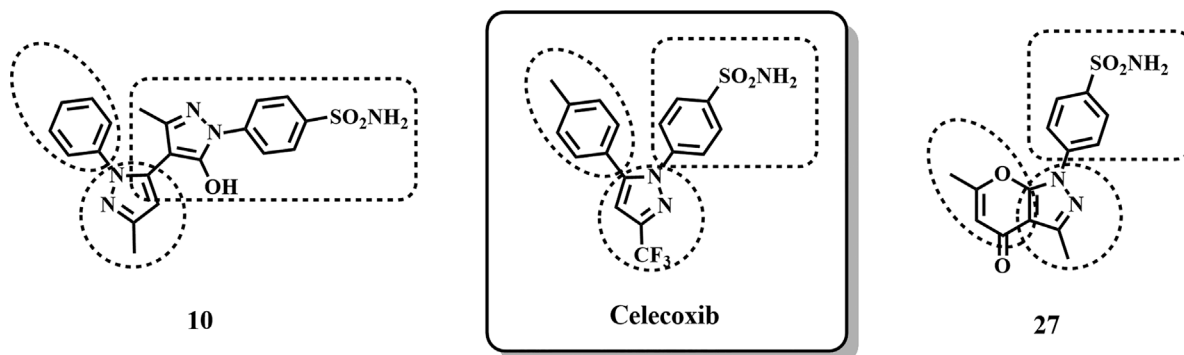


Figure 2. Structures of celecoxib (selective COX-2 inhibitor) and the most active anti-inflammatory compounds **10** and **27**.

inflammatory potential as compared with the parent analog **5**, being almost equipotent with indomethacin and celecoxib. Yet, introduction of Cl or COCF₃ moieties at position-5 of the pyrano[2,3-c]pyrazole ring system as in **29** and **33** resulted in an obvious drop in the biological activity.

In vitro COX-1 and COX-2 inhibitory assay

All the developed 27 target compounds (**4–27**, **29**, **32**, and **33**) were evaluated for their ability to *in vitro* inhibit COX-1 and COX-2 isozymes employing an ovine COX-1/COX-2 inhibitor screening assay kit (Catalog No. 760111, Cayman Chemicals Inc., Ann Arbor, MI, USA) according to the manufacturer's instructions and a literature procedure [37, 38]. The method relied on the peroxidase component of COX which is assayed colorimetrically by monitoring the appearance of oxidized *N,N,N',N'*-tetramethyl-1,4-phenylenediamine (TMPD), that is generated during the reduction of PGG₂ to PGH₂, at 590 nm. The efficiencies of the investigated compounds were measured as the concentration causing 50% enzyme inhibition (IC₅₀; μM), the selectivity index (SI value) was calculated as IC₅₀ (COX-1)/IC₅₀ (COX-2).

The results recorded in Table 2 indicated that all the tested compounds showed mild inhibitory effects on the activity of COX-1 (IC₅₀ range 5.64–12.2 μM) as compared with indomethacin (IC₅₀ 3.54 μM), while they proved to be moderate to good COX-2 inhibitors (IC₅₀ values range 0.72–2.74 μM), when correlated to celecoxib (IC₅₀ 0.84 μM), except the analogs **11**, **12**, **26**, **29**, and **33** (IC₅₀ > 3 μM). In particular, compounds **10** and **27** exerted COX-2 inhibition (IC₅₀ 0.72 and 0.76 μM,

respectively) superior to that of celecoxib (IC₅₀ 0.84 μM), whereas the activity of the analog **17** (IC₅₀ 0.91 μM) was nearly equiactive to celecoxib. Furthermore, most of the investigated compounds displayed considerable COX-2 selectivity index values (SI) lying between 2.04 and 7.83, when compared with celecoxib (SI value 8.68). Prominently, compounds **10**, **17**, and **27** were found to be obviously selective COX-2 inhibitors (SI values 7.83, 6.87, and 7.16, respectively), while the analogs **5** and **19** revealed moderate selectivity towards the same isozyme (SI values 6.15 and 5.27, respectively). The rest of the tested compounds showed mild to weak selectivity indices with SI values range lying between 2.04 and 3.93.

Collectively, the *in vivo* ED₅₀ values for the most potent five derivatives **5**, **10**, **17**, **19**, and **27** get along with their *in vitro* COX-2 selectivity indices, suggesting their usefulness as selective anti-inflammatory COX-2 inhibitors. The bipyrazole **10** and pyranopyrazole **27** (structurally relevant to celecoxib) could be considered as the most active anti-inflammatory members in this study, being more potent than indomethacin and nearly equiactive to celecoxib, besides their obvious selective COX-2 inhibitory activity.

Ulcerogenic effect

Compounds that showed remarkable *in vivo* and *in vitro* anti-inflammatory potential (**5**, **10**, **17**, **19**, and **27**) were further investigated for their ulcerogenic liability in rats [39]. The results denoted that all the five tested compounds revealed eminent gastrointestinal (GI) safety profiles (0–20% ulceration) in the population of the test animals at oral doses of

Table 2. *In vitro* COX-1/COX-2 enzymatic inhibition assay of the active compounds.^{a)}

Compound number	COX-1 IC ₅₀ (μM) ^{b)}	COX-2 IC ₅₀ (μM) ^{c)}	COX-2 SI ^{d)}
Indomethacin	3.54	3.73	0.95
Celecoxib	7.29	0.84	8.68
4	8.96	2.08	4.31
5	7.63	1.24	6.15
7	8.58	1.73	4.96
9	10.1	2.47	4.09
10	5.64	0.72	7.83
11	9.26	3.01	3.08
12	8.48	3.38	2.51
13	5.93	1.51	3.93
16	6.34	1.97	3.21
17	7.55	0.91	6.87
18	9.23	2.55	3.62
19	7.48	1.42	5.27
20	9.89	2.66	3.72
24	9.48	2.74	3.46
26	10.4	3.11	3.35
27	9.41	0.76	7.16
29	8.51	4.17	2.04
33	12.2	5.01	2.43

^{a)} Values obtained using an ovine COX assay kit (Catalog No. 760111, Cayman Chemical, Inc., Ann Arbor, MI, USA).

^{b,c)} Compounds' concentrations causing 50% inhibition of COX-1 and COX-2, respectively. Results are the mean of two readings.

^{d)} COX-2 selectivity index: (COX-1 IC₅₀/COX-2 IC₅₀).

30 $\mu\text{mol/kg}$ per day, as compared with indomethacin (100% ulceration) and celecoxib (40% ulceration), the reference anti-inflammatory drugs utilized in the present study (Table 1). It is to be noted that, although the analogs **10** and **27** displayed equipotent or even higher anti-inflammatory profiles than indomethacin, yet they kept their GI safety properties (20 and 0% ulceration, respectively). Gross observation of the isolated rat stomachs showed a normal stomach texture for compounds **17**, **19**, and **27** (0% ulceration), whereas the analogs **10** and **27** exhibited slight hyperemia (20% ulceration).

Acute toxicity

The same biologically active derivatives **5**, **10**, **17**, **19**, and **27** were further investigated for their oral acute toxicity in male mice according to the method described by Litchfield and Wilcoxon [40]. The obtained acute lethal doses (ALD₅₀) indicated that the test compounds proved to be nontoxic and well tolerated by experimental animals up to 250 mg/kg. Moreover, the same compounds were tested for their toxicity through the parenteral route [41], where they proved to be non-toxic up to 80 mg/kg.

In silico studies

In silico calculation of the pharmacokinetic properties (ADME-T) and drug-likeness

Drug-likeness is a term that describes an integrated equilibrium between multiple molecular properties and structure features that define whether a particular compound is comparable to already known drugs. Among the common principles applied to evaluate the drug-like properties of a compound, stemmed prominently the Lipinski's rule of 5 (RO5) [42] and Veber's criteria [43]. These properties comprise hydrophobicity, electronic distribution, hydrogen-bonding capability, molecule size, and flexibility that would affect molecule's behavior in a living system including bioavailability, transport properties, affinity to proteins, reactivity, and toxicity.

In this context, a computational study for the most biologically active compounds **5**, **10**, **17**, **19**, and **27** utilizing the Molinspiration online property calculation toolkit [44] was carried out to determine the Lipinski's molecular properties and the number of rotatable bonds (nROTB), together with the topographical polar surface area (TPSA; a sum of polar atoms' surfaces: A descriptor for drug absorption, penetrability and bioavailability), the percentage of absorption (ABS%) calculated as $(\text{ABS}\% = 109 - 0.345 \times \text{TPSA})$ [45] and the molecular volume (a determinant of the transport characteristics).

The results presented in Table 3 revealed that all the tested compounds comply with Lipinski's rule of 5, where $\log P$ values ranged between 0.17 and 2.03 (<5), MW range 307–409 (<500), HBA range 5–8 (≤ 10), and HBD range 1–3 (<5), suggesting that these compounds would not be expected to cause problems with oral bioavailability. Moreover, all the tested compounds showed nROTB values of 2–5 (<10), indicating acceptable molecular flexibility with consequent

expected good permeability and oral bioavailability. Additionally, all the evaluated compounds showed TPSA range 55.88–132.36 \AA^2 ($<140 \text{\AA}^2$), indicating good permeability and transport of the compounds in the cellular plasma membrane. Furthermore, all the tested compounds exhibited a considerable % ABS range 63.3–89.7%, which is a designation of good bioavailability upon oral administration. It is to be noted that TPSA is inversely proportional to %ABS, for example, the analog **17** possesses the maximum absorption (89.7%), whereas its corresponding TPSA was the least among the series (55.88 \AA^2).

On the other hand, the OSIRIS Property Explorer (2014: Version 2) software [46] was utilized to calculate the aqueous solubility ($\log S$) of the tested compounds (being significantly affecting absorption as well as distribution characteristics), where they gave moderate $\log S$ values ranging between -1.96 and -4.63 mol/L. Finally, the same OSIRIS software was employed to determine the overall and drug score values which is an expression representing integration of drug-likeness, several physicochemical parameters, and toxicity probabilities in one numerical value that can be utilized to foresee compound's ability to act as a drug candidate. A positive value for drug-likeness and drug score indicates that the compound contains fragments that are often present in most of currently used drugs. The results revealed that compounds **10**, **17**, **19**, and **27** gave positive values for drug-likeness lying between 4.48 and 6.79, while the analog **5** showed negative value of drug-likeness (-2.85). Additionally, all the evaluated compounds (including those compounds with negative drug-likeness scores) have displayed positive values ranging from 0.14 to 0.66 in the drug score calculation (Table 3). Finally, according to OSIRIS findings, prediction of the expected toxicity risks pointed out that none of the five investigated compounds would exert tumorigenic, mutagenic, irritant, or reproductive toxicity.

Conclusion

The objective of the present research work was to develop a series of novel non-acidic polysubstituted pyrazoles to be evaluated for their *in vivo* and *in vitro* anti-inflammatory activities. Our aim has been verified by the synthesis of 27 structure hybrids comprising basically the 5-hydroxy-3-methyl-1-phenyl-4-substituted-1*H*-pyrazole scaffold directly attached to a variety of non-acidic heterocycles and functionalities or annulated as pyrano[2,3-*c*]pyrazoles for synergistic purpose. In general, obvious anti-inflammatory activity was linked with analogs comprising a sulfonamido functionality and/or the pyrazolyl, pyrimidinyl, and tetrazolo[1,5-*a*]pyrimidinyl counterparts, in addition to the pyrano[2,3-*c*]pyrazole structure variant. Eighteen compounds were able to exert variable *in vivo* anti-inflammatory activities, among which the analogs **5**, **10**, **17**, **19**, and **27** proved to be the most active candidates as evidenced from their distinctive % protection values which were comparable or even better than the

Table 3. *In silico* ADME-T calculations, Lipinski's parameters drug-likeness, and drug score^{a,b,c)1} of the biologically active compounds.

Compound number	Logp ^{c)}	MW ^{d)}	HBA ^{e)}	HBD ^{f)}	Viol. ^{g)}	nROTB ^{h)}	TPSA ⁱ⁾	% ABS ^{j)}	Vol. ^{k)}	LogS ^{l)}	D.L. ^{m)}	D.S. ⁿ⁾
5	0.17	337.35	8	3	0	5	132.36	63.33	275.29	-2.72	-2.85	0.14
10	2.03	409.47	8	3	0	4	116.04	68.97	344.55	-3.73	5.68	0.46
17	1.96	312.40	5	1	0	2	55.88	89.70	274.84	-1.96	6.34	0.66
19	1.59	307.32	8	1	0	2	90.04	77.94	261.94	-3.14	4.48	0.59
27	0.78	319.34	7	2	0	2	108.20	71.67	257.05	-4.63	6.79	0.37
Ind. ^{o)}	4.08	343.77	5	1	0	4	68.54	85.35	286.68	-5.40	9.41	0.56
Cel. ^{p)}	3.61	381.38	5	2	0	4	77.99	82.09	298.65	-4.17	8.11	0.37

^{a)} Molinspiration chemoinformatics property calculator (2014).

^{b)} OSIRIS property explorer (2014).

^{c)} Partition coefficient.

^{d)} Molecular weight.

^{e)} Number of H-Bond acceptors (O and N atoms).

^{f)} Number of H-Bond donors (OH and NH groups).

^{g)} Number of Rule of 5 violations.

^{h)} Number of rotatable bonds.

ⁱ⁾ Topological polar surface area.

^{j)} Absorption %.

^{k)} Molecular volume.

^{l)} Aqueous solubility prediction.

^{m)} Drug likeness.

ⁿ⁾ Drug score.

^{o)} Indomethacin.

^{p)} Celecoxib.

reference standards. The ED₅₀ values of the most active analogs **5**, **10**, **17**, **19**, and **27** (35.7–75.2 μmol/kg) affirmed the anti-inflammatory potential, especially the bipyrazole **10** (ED₅₀ 35.7 μmol/kg) which was nearly equiactive with celecoxib (32.1 μmol/kg). Meanwhile, all the tested compounds showed *in vitro* mild COX-1 inhibitory effects, while they proved to be moderate to good COX-2 inhibitors. In particular, **10**, **17**, and **27** exhibited distinctive COX-2 inhibition (IC₅₀ 0.72, 0.91 and 0.76 μM, respectively) as compared with celecoxib (IC₅₀ 0.84 μM), meanwhile they possessed noticeable COX-2 selectivity (SI values 7.83, 6.87, and 7.16, respectively), close to that of celecoxib (SI 8.68). Additionally, **5**, **10**, **17**, **19**, and **27** proved to be GI safe (0–20% ulceration), and non-toxic being well tolerated the by experimental animals up to 250 mg/kg orally and 80 mg/kg parenterally. Collectively, the *in vivo* ED₅₀ values for the most potent five derivatives get along with their *in vitro* COX-2 selectivity indices, suggesting their usefulness as selective anti-inflammatory COX-2 inhibitors. The bipyrazole **10** and pyranopyrazole **27** (structurally relevant to celecoxib) could be considered the most active anti-inflammatory members in this study, being more potent than indomethacin and nearly equiactive to celecoxib, besides their obvious selective COX-2 inhibitory activity, high safety margin, and predicted pharmacokinetic (ADME-T) suitability for oral use.

Consequently, such type of hybrid structures would represent the appropriate matrix for future development

of a new class of non-acidic anti-inflammatory agents that deserves further investigation and derivatization.

Experimental

Chemistry

General

Melting points were determined on a Gallenkamp melting point apparatus and are uncorrected. The infrared (IR) spectra were recorded on Shimadzu FT-IR 8400S infrared spectrophotometer using the KBr pellet technique. ¹H and ¹³C NMR spectra were recorded on a Bruker DPX-400 FT NMR spectrometer using tetramethylsilane as the internal standard and CDCl₃ as a solvent (chemical shifts in δ, ppm). Splitting patterns were designated as follows: *s*: singlet; *d*: doublet; *m*: multiplet; *q*: quartet. Elemental analyses were performed on a 2400 Perkin Elmer Series 2 analyzer and the found values were within ±0.4% of the theoretical values. Follow-up of the reactions and checking the homogeneity of the compounds were made by TLC on silica gel-protected aluminum sheets (Type 60 F254, Merck) and the spots were detected by exposure to UV-lamp at λ 254 nm. Most of the starting compounds and target products were synthesized according to known literature procedures [47–49]. The synthesis and mechanism of formation of compound **20** was carried out following the method described by Faidallah et al. [34].

Selected NMR spectra as well as the InChI codes of the investigated compounds together with some biological activity data are provided as Supporting Information.

General procedure for the synthesis of 4-hydroxy-6-methyl-3-[1-(substituted hydrazono)ethyl]pyran-2-ones 2 and 3

To a solution of dehydroacetic acid (DHA) **1** (1.68 g, 10 mmol) in benzene (20 mL) was added the appropriate aryl hydrazine (10 mmol). The mixture was refluxed for 15 min and allowed to stand at room temperature for 2 h. After being cooled, the hydrazone was collected by filtration and recrystallized from ethanol. Physicochemical and analytical data are recorded in Table 4 (see the Supporting Information for an extended version of Table 4).

IR (cm⁻¹) of compounds **2** and **3**: 1705–1712 (CO), 3298–3323 (OH), 3638–3456 (NH), 1157, 1360 (SO₂N for compound

3). ¹H NMR (δ-ppm) of compound **2**: 2.14 (s, 3H, CH₃), 2.71 (s, 3H, CH₃), 5.80 (s, 1H, H-5), 7.06–7.65 (m, 6H, ArH + NH), 16.52 (exchangeable OH). ¹³C NMR (δ-ppm) of compound **2**: 16.95 (CH₃), 20.27 (CH₃), 95.58, 102.83, 115.45, 118.56, 129.32, 144.15, 146.47, 171.35 (Ar-C), 163.66 (CN), 179.53 (CO). ¹H NMR (δ-ppm) of compound **3**: 2.46 (s, 3H, CH₃), 2.56 (s, 3H, CH₃), 5.63 (s, 1H, H-5), 7.13–7.74 (m, 7H, ArH + NH + NH₂), 16.48 (exchangeable OH). ¹³C NMR (δ-ppm) of compound **3**: 17.54 (CH₃), 20.23 (CH₃), 96.45, 103.64, 115.73, 126.28, 129.35, 141.41, 149.94, 174.23, 162 (ArC), 161.96 (CN), 178.86 (CO).

General procedure for the synthesis of 1-(5-hydroxy-3-methyl-1-(4-substituted phenyl)-1H-pyrazol-4-yl)butane-1,3-diones 4 and 5

A solution of the appropriate hydrazono derivative **2** or **3** (10 mmol) in acetic acid (20 mL) was refluxed for 1 h. The reaction mixture was concentrated, cooled, and the formed

Table 4. Physicochemical and analytical data^{a)} for compounds **2**–**33**.

Compound number	R	Yield (%)	m.p. (°C)	Mol. formula (mol. weight)
2	H	70	198–200	C ₁₄ H ₁₄ N ₂ O ₃ (258.28)
3	SO ₂ NH ₂	79	222–224	C ₁₄ H ₁₅ N ₃ O ₅ S (337.35)
4	H	91	201–202	C ₁₄ H ₁₄ N ₂ O ₃ (258.28)
5	SO ₂ NH ₂	85	214–216	C ₁₄ H ₁₅ N ₃ O ₅ S (337.35)
6	H	86	136–138	C ₂₀ H ₁₈ BrN ₃ O ₂ (412.28)
7	SO ₂ NH ₂	92	324–326	C ₂₀ H ₁₉ BrN ₄ O ₄ S (491.36)
8	H	67	126–128	C ₁₄ H ₁₃ N ₃ O ₂ (255.27)
9	SO ₂ NH ₂	92	324–326	C ₁₄ H ₁₄ N ₄ O ₄ S (334.35)
10	–	75	312–314	C ₂₀ H ₁₉ N ₅ O ₃ S (409.46)
11	–	77	143–145	C ₂₇ H ₂₂ ClN ₅ O ₃ S (532.01)
12	–	73	242–244	C ₂₇ H ₂₃ ClN ₆ O ₄ S (563.03)
13	–	72	225–227	C ₂₇ H ₂₃ ClN ₆ O ₃ S ₂ (579.09)
14	–	66	164–166	C ₂₉ H ₂₃ ClN ₆ O ₄ S ₂ (619.11)
15	–	70	174–176	C ₃₅ H ₂₇ ClN ₆ O ₃ S ₂ (679.21)
16	H	71	163–165	C ₁₅ H ₁₄ N ₄ OS (298.36)
17	CH ₃	66	145–147	C ₁₆ H ₁₆ N ₄ OS (312.39)
18	–	75	185–187	C ₁₅ H ₁₆ N ₆ O (296.33)
19	–	67	250–252	C ₁₅ H ₁₃ N ₇ (307.31)
20	–	60	201–203	C ₁₇ H ₁₆ N ₆ O (320.35)
21	–	59	222–224	C ₁₇ H ₁₅ BrN ₆ O (399.24)
22	–	67	250–252	C ₁₉ H ₁₈ N ₆ O ₃ (378.38)
23	–	70	134–136	C ₁₇ H ₁₄ N ₆ O ₃ (350.33)
24	CH ₃	65	272–274	C ₁₈ H ₁₈ N ₆ O (334.38)
25	C ₆ H ₅	68	230–232	C ₂₃ H ₂₀ N ₆ O (396.44)
26	H	72	152–154	C ₁₄ H ₁₂ N ₂ O ₂ (240.26)
27	SO ₂ NH ₂	68	272–274	C ₁₄ H ₁₃ N ₃ O ₄ S (319.34)
29	–	74	145–147	C ₁₄ H ₁₁ ClN ₂ O ₂ (274.70)
32	H	72	148–150	C ₁₆ H ₁₁ F ₃ N ₂ O ₃ (336.27)
33	SO ₂ NH ₂	67	286–288	C ₁₆ H ₁₂ F ₃ N ₃ O ₅ S (415.34)

^{a)} The found values in the elementary microanalysis are within ±0.4% of the calculated values.

precipitate was filtered, washed with water, dried, and recrystallized from ethanol. Physicochemical and analytical data are recorded in Table 4.

IR (cm⁻¹) of **4** and **5**: 1622–1635 (CO), 1715–1724 (CO), 3328–3398 (OH), 1149, 1355 (SO₂N for compound **4**). ¹H NMR (δ-ppm) of compound **4**: 2.11 (s, 3H, CH₃), 2.34 (s, 3H, CH₃), 3.88 (s, 2H, CH₂), 7.26–7.80 (m, ArH, 5H), 14.85 (exchangeable OH). ¹³C NMR (δ-ppm) of compound **4**: 15.50 (CH₃), 22.24 (CH₃), 30.66 (CH₂), 96.82, 100.40, 120.40, 121.37, 126.77, 126.83, 129.96, 129.06, 137.03, 147.12, 158.37 (ArC), 181.25 (CO), 188.58 (CO). ¹H NMR (δ-ppm) of compound **5**: 2.56 (s, 3H, CH₃), 2.43 (s, 3H, CH₃), 3.97 (s, 2H, CH₂), 7.64–7.84 (m, 6H, ArH + NH₂), 15.28 (exchangeable OH). ¹³C NMR (δ-ppm) of compound **5**: 16.0 (CH₃), 22.45 (CH₃), 30.18 (CH₂), 96.64, 100.44, 120.98, 121.57, 126.73, 126.38, 129.42, 129.97, 137.24, 147.71, 157.95 (ArC), 180.43 (CO), 188.25 (CO).

*General procedure for the synthesis of 3-((2-bromophenyl)-amino)-1-(5-hydroxy-3-methyl-1-(4-substituted phenyl)-1H-pyrazol-4-yl)but-2-en-1-ones **6** and **7***

A solution of the appropriate pyrazole **4** or **5** (10 mmol) in ethanol (20 mL) was refluxed with the 2-bromoaniline (1.7 g, 10 mmol) for 2 h. The reaction mixture was cooled and the precipitated aryl aminopyrazole derivative was filtered, washed with ethanol, and recrystallized from DMF. Physicochemical and analytical data are recorded in Table 4.

IR (cm⁻¹) of **6** and **7**: 1662–1679 (CO), 3265–3320 (OH), 3395–3405 (NH), 1156, 1372 (SO₂N for compound **7**). ¹H NMR (δ-ppm) of compound **6**: 2.45 (s, 3H, CH₃), 2.18 (s, 3H, CH₃), 5.46 (s, 1H, CH=), 7.18–7.86 (m, 11H, ArH + NH), 12.26 (exchangeable OH). ¹³C NMR (δ-ppm) of compound **6**: 15.43 (CH₃), 20.44 (CH₃), 94.28 (CH=) 100.42, 117.32, 120.28, 126.13, 129.53, 129.46, 131.66, 136.75, 137.90, 146.86, 159.74, 161.44 (ArC), 184.86 (CO). ¹H NMR (δ-ppm) of compound **7**: 2.33 (s, 3H, CH₃), 2.43 (s, 3H, CH₃), 5.65 (s, 1H, CH=), 7.09–7.79 (m, 11H, ArH + NH + NH₂), 12.56 (exchangeable OH). ¹³C NMR (δ-ppm) of compound **7**: 15.84 (CH₃), 20.82 (CH₃), 94.38 (CH=) 100.76, 117.34, 120.48, 126.59, 129.43, 129.56, 131.23, 136.94, 137.93, 146.55, 160.47, 161.32 (ArC), 184.52 (CO).

*General procedure for the synthesis of 5-hydroxy-3-methyl-4-(3-methylisoxazol-5-yl)-1-(4-substituted phenyl)-1H-pyrazoles **8** and **9***

A solution of the appropriate pyrazole **4** or **5** (10 mmol) and hydroxyl amine hydrochloride (0.69 g, 10 mmol) in a mixture of ethanol and acetic acid (1:1, 20 mL) was refluxed for 2 h. The reaction mixture was allowed to attain room temperature then allowed to stand in the refrigerator for further 12 h. The solid thus precipitated was collected by filtration and recrystallized from ethanol. Physicochemical and analytical data are recorded in Table 4.

IR (cm⁻¹) of **8** and **9**: 3345–3378 (OH), 1152, 1368 (SO₂N for compound **9**). ¹H NMR (δ-ppm) of compound **8**: 2.09 (s, 3H, CH₃), 2.47 (s, 3H, CH₃), 6.33 (s, 1H, isoxazole C₄-H), 7.04–7.88 (m, ArH, 5H), 14.62 (exchangeable OH). ¹³C NMR (δ-ppm) of

compound **8**: 13.96 (CH₃), 19.55 (CH₃), 96.42, 106.78, 112.59, 120.99, 127.31, 129.44, 137.08, 146.77, 153.57, 161.65 (ArC). ¹H NMR (δ-ppm) of compound **9**: 2.61 (s, 3H, CH₃), 2.98 (s, 3H, CH₃), 6.18 (s, 1H, isoxazole C₄-H), 7.22–7.75 (m, ArH, 4H), 14.83 (exchangeable OH). ¹³C NMR (δ-ppm) of compound **9**: 13.44 (CH₃), 19.23 (CH₃), 96.67, 106.34, 112.95, 120.46, 127.22, 129.76, 137.16, 146.83, 153.36, 161.83 (ArC).

*5-Hydroxy-3-methyl-1-(4-sulfamylphenyl)-4-(3-methyl-1-phenyl-1H-pyrazol-5-yl)-1H-pyrazole **10***

A solution of the starting pyrazole **5** (3.3 g, 10 mmol) in ethanol (20 mL) was refluxed with phenylhydrazine (1.1 g, 10 mmol) for 2 h. The reaction mixture was cooled and the formed precipitate was filtered, washed with ethanol, dried, and recrystallized from ethanol. Physicochemical and analytical data are recorded in Table 4.

IR (cm⁻¹): 3342 (OH), 3405 (NH), 1153, 1376 (SO₂N), 3349, 3355 (NH₂). ¹H NMR (δ-ppm): 2.38 (s, 3H, CH₃), 2.79 (s, 3H, CH₃), 6.14 (s, 1H, pyrazole C₄-H), 7.13–7.69 (m, 11H, ArH + NH₂), 13.54 (s, 1H, exchangeable OH). ¹³C NMR (δ-ppm): 11.76 (CH₃), 14.09 (CH₃), 95.82, 101.38, 112.74, 120.28, 125.52, 128.84, 138.57, 140.39, 145.48, 146.58 (ArC).

*5-Hydroxy-3-methyl-1-[4-(N-4-chlorobenzylidenesulfamyl)-phenyl]-4-(3-methyl-1-phenyl-1H-pyrazol-5-yl)-1H-pyrazole **11***

A stirred solution of the bipyrazole **10** (4.1 g, 10 mmol) in acetic acid (25 mL) was heated under reflux with 4-chlorobenzaldehyde (1.4 g, 10 mmol) for 8 h. The reaction mixture was concentrated and the separated azomethine was filtered, dried, and recrystallized from the ethanol. Physicochemical and analytical data are recorded in Table 4.

IR (cm⁻¹): 3352 (OH), 1150, 1345 (SO₂N). ¹H NMR (δ-ppm): 2.12 (s, 3H, CH₃), 2.58 (s, 3H, CH₃), 6.36 (s, 1H, pyrazole, C₄-H), 7.21–7.55 (m, 13H, ArH), 8.21 (s, 1H, CH=N), 15.24 (s, 1H, exchangeable OH). ¹³C NMR (δ-ppm): 15.61 (CH₃), 20.44 (CH₃), 94.89, 100.74, 113.32, 117.52, 120.15, 122.65, 126.60, 127.58, 128.82, 129.25, 129.17, 130.31, 137.81, 139.66, 146.52, 147.23, 158.69, 160.32 (ArC), 161.24 (CH=N).

*N1-[4-(3-Methyl-1-phenyl-1H-pyrazol-5-yl)-5-hydroxy-5-methyl-1H-pyrazol-1-yl]benzenesulfonyl-N3-(4-chlorophenyl)urea **12***

A stirred mixture of the bipyrazole **10** (4.1 g, 10 mmol), anhydrous K₂CO₃ (1.4 g, 10 mmol), and 4-chlorophenyl isocyanate (1.5 g, 10 mmol) in dry acetone (25 mL) was heated under reflux for 18 h. The solvent was removed under reduced pressure and the remaining solid residue was dissolved in water (30 mL). After neutralization of the resulting solution with drops of 2 N HCl, the precipitated crude product was filtered, washed with water, dried, and recrystallized from ethanol. Physicochemical and analytical data are recorded in Table 4.

IR (cm⁻¹): 1652 (CO), 1336, 1164 (SO₂N), 3343 (OH), 3402 (NH). ¹H NMR (δ-ppm): 2.11 (s, 3H, CH₃), 2.48 (s, 3H, CH₃), 6.57 (s, 1H, pyrazole C₄-H), 7.11–7.86 (m, 15H, ArH + 2NH), 12.06

(s, 1H, exchangeable OH). ^{13}C NMR (δ -ppm): 15.79 (CH₃), 20.28 (CH₃), 97.16, 101.49, 101.65, 114.49, 123.61, 123.87, 130.22, 130.94, 138.67, 143.18, 147.81, 160.37, 161.29, 162.14, 165.19, 169.10 (ArC), 173.75 (CO).

N1-[4-(3-Methyl-1-phenyl-1H-pyrazol-5-yl)-5-hydroxy-5-methyl-1H-pyrazol-1-yl]benzenesulfonyl-N₃-(4-chlorophenyl)thiourea 13

A solution of 4-chlorophenyl isothiocyanate (1.7 g, 10 mmol) in dry acetone (5 mL) was added to a stirred mixture of the bipyrazole **10** (4.1 g, 10 mmol) and anhydrous K₂CO₃ (1.4 g, 10 mmol) in dry acetone (25 mL), and the mixture was heated under reflux for 10 h. Working up of the reaction mixture was done as mentioned above for compound **12**. The crude product was recrystallized from DMF. Physicochemical and analytical data are recorded in Table 4.

IR (cm⁻¹): 1155 (CS), 1181, 1368, 1169 (SO₂N), 3358 (OH), 3402 (NH). ^1H NMR (δ -ppm): 2.09 (s, 3H, CH₃), 2.47 (s, 3H, CH₃), 6.59 (s, 1H, pyrazole C₄-H), 7.04–7.88 (m, 15H, ArH + 2NH), 11.86 (s, 1H, exchangeable OH). ^{13}C NMR (δ -ppm): 15.92 (CH₃), 20.08 (CH₃), 94.87, 100.92, 120.53, 120.98, 122.73, 123.29, 126.03, 160.02, 160.99 (ArC), 184.80 (CS).

2-[[4-(3-Methyl-1-phenyl-1H-pyrazol-5-yl)-5-hydroxy-5-methyl-1H-pyrazol-1-yl]benzenesulfonylimino]-3-(4-chlorophenyl)thiazolidin-4-one 14

To a stirred solution of the sulfonylthioureido derivative **13** (3.0 g, 5 mmol) in absolute ethanol (20 mL) was added ethyl bromoacetate (1.84 g, 11 mmol) and anhydrous sodium acetate (1.64 g, 0.02 mol) and the mixture was heated under reflux for 2 h. The reaction mixture was left for 1 h to attain room temperature, then poured onto ice water (30 mL). The solid product thus formed was filtered, washed with water, dried, and recrystallized from ethanol/benzene mixture (1:1). Physicochemical and analytical data are recorded in Table 4.

IR (cm⁻¹): 1329, 1156 (SO₂N), 1712 (CO), 3397 (OH). ^1H NMR (δ -ppm): 2.51 (s, 3H, CH₃), 2.42 (s, 3H, CH₃), 3.42 (s, 2H, thiazolidine CH₂), 5.48 (s, 1H, pyrazole C₄-H), 7.32–7.76 (m, 13H, ArH), 14.44 (s, 1H, exchangeable OH). ^{13}C NMR (δ -ppm): 17.53 (CH₃), 20.04 (CH₃), 37.32 (CH₂), 96.95, 107.37, 115.29, 115.50, 121.58, 121.38, 124.84, 126.24, 127.72, 127.32, 128.38, 140.61, 140.63, 140.92, 161.25, 163.74, 163.32, 163.73 (ArC), 172.47 (C=N), 184.77 (CO).

2-[[4-(3-Methyl-1-phenyl-1H-pyrazol-5-yl)-5-hydroxy-5-methyl-1H-pyrazol-1-yl]benzenesulfonylimino]-4-phenyl-3-(4-chlorophenyl)thiazoline 15

A solution of the sulfonylthioureido **13** (3.0 g, 10 mmol) in absolute ethanol (20 mL) was refluxed with phenacyl bromide (2.2 g, 11 mmol) and anhydrous sodium acetate (1.64 g, 20 mmol) for 2 h, during which a solid product was partially crystallized out. The mixture was left to attain room temperature, filtered, washed with cold ethanol, dried, and recrystallized from ethanol. Physicochemical and analytical data are recorded in Table 4.

IR (cm⁻¹): 1336, 1166 (SO₂N), 3328 (OH). ^1H NMR (δ -ppm): 2.15 (s, 3H, CH₃), 2.42 (s, 3H, CH₃), 5.63 (s, 1H, thiazoline C₅-H), 6.42 (s, 1H, pyrazole C₄-H), 6.68–7.46 (m, 18H, ArH), 14.44 (s, 1H, exchangeable OH). ^{13}C NMR (δ -ppm): 15.71 (CH₃), 20.89 (CH₃), 97.78, 110.87, 114.24, 120.02, 121.65, 126.04, 126.92, 128.54, 129.12, 129.29, 129.44, 129.94, 136.37, 136.62, 139.85, 142.40, 153.64, 155.76 (ArC), 169.32 (N=C).

6-(5-Hydroxy-3-methyl-1-phenyl-1H-pyrazol-4-yl)-4-methyl-1-substituted-1H-pyrimidine-2-thiones 16 and 17

A solution of the pyrazole **4** (2.58 g, 10 mmol) in absolute ethanol (20 mL) was refluxed with the appropriate thiourea (10 mmol) for 6 h. The reaction mixture was concentrated and the separated solid product was filtered, washed with ethanol and recrystallized from ethanol/DMF (5:1). Physicochemical and analytical data are recorded in Table 4.

IR (cm⁻¹): of compounds **16** and **17**: 3322–3356 (OH), 1182–1192 (CS), 3375 (NH for compound **16**). ^1H NMR (δ -ppm) of compound **16**: 2.16 (s, 3H, CH₃), 2.58 (s, 3H, CH₃), 5.76 (s, 1H, exchangeable NH), 7.11–7.43 (m, 6H, Ar H + pyrimidine C₅-H), 15.85 (s, 1H, exchangeable OH). ^{13}C NMR (δ -ppm) of compound **16**: 19.99 (CH₃), 20.31 (CH₃), 97.58, 107.10, 126.94, 129.86, 134.02, 134.93, 163.32, 163.73, 165.03 (ArC), 185.02 (C=S). ^1H NMR (δ -ppm) of compound **17**: 1.72 (s, 3H, CH₃), 2.45 (s, 3H, CH₃), 2.76 (s, 3H, CH₃), 6.89–7.49 (m, 6H, Ar H + pyrimidine C₅-H), 15.12 (s, 1H, exchangeable OH). ^{13}C MR (δ -ppm) of compound **17**: 19.62 (CH₃), 20.63 (CH₃), 37.22 (CH₃), 99.8, 108.2, 118.7, 126.0, 129.1, 129.3, 139.8, 152.4, 157.9, 164.8 (ArC), 180.40 (C=S).

6-(5-Hydroxy-3-methyl-1-phenyl-1H-pyrazol-4-yl)-2-hydrazino-4-methylpyrimidine 18

A solution of the pyrimidine-2-thione **16** (1.5 g, 5 mmol) and 98% hydrazine hydrate (1 g) in absolute ethanol (50 mL) was stirred at room temperature for 2 h. The solid which was separated during stirring was filtered and recrystallized from ethanol. Physicochemical and analytical data are recorded in Table 4.

IR (cm⁻¹): 3192–3342 (NHNH₂), 3367 (OH). ^1H NMR (δ -ppm): 1.72 (s, 3H, CH₃), 2.38 (s, 3H, CH₃), 5.92 (s, 2H, exchangeable NH₂), 6.14 (s, 1H, exchangeable NH), 6.69–7.38 (m, 6H, ArH + H-5), 14.79 (s, 1H, exchangeable OH). ^{13}C NMR (δ -ppm): 10.03 (CH₃), 18.2 (CH₃), 99.8, 108.2, 118.7, 126.0, 129.1, 129.3, 139.8, 152.4, 157.9, 164.8 (ArC).

*5-(5-Hydroxy-3-methyl-1-phenyl-1H-pyrazol-4-yl)-7-methyl-[1,2,3,4]tetrazolo[1,5-*a*]pyrimidine 19*

A stirred solution of the hydrazino derivative **18** (2.9 g, 10 mmol) in glacial acetic acid (10 mL) was gradually treated with 25% aqueous NaNO₂ (15 mL) at room temperature. The tetrazolo derivative which separated as white solid was filtered, washed with water, and recrystallized from DMF. Physicochemical and analytical data are recorded in Table 4.

IR (cm⁻¹): 3356 (OH). ^1H NMR (δ -ppm): 2.15 (CH₃), 2.57 (CH₃), 6.95–7.26 (m, 6H, ArH + H-5), 15.58 (s, 1H, exchangeable OH). ^{13}C NMR (δ -ppm): 19.95 (CH₃), 20.26 (CH₃), 97.26, 107.27,

114.76, 126.74, 129.07, 139.27, 147.53, 159.19, 163.28, 163.60, 166.56 (ArC).

5-(5-Hydroxy-3-methyl-1-phenyl-1H-pyrazol-4-yl)-3,7-dimethyl[1,2,4]triazolo[3,4-a]pyrimidine 20

A mixture of the hydrazino derivative **18** (2.9 g, 10 mmol) and acetylacetone (1.0 g, 10 mmol) in ethanol (20 mL) was refluxed with stirring for 8 h. The reaction mixture was concentrated and the separated product was filtered, washed, dried, and recrystallized from ethanol. Physicochemical and analytical data are recorded in Table 4.

IR (cm⁻¹): 3375 (OH). ¹H NMR (δ-ppm): 2.10, (s, 3H, CH₃), 2.36 (s, 3H, CH₃), 2.74 (s, 3H, CH₃), 7.04–7.88 (m, 5H, ArH), 5.33 (s, 1H, C₆-H), 11.86 (s, 1H, exchangeable OH). ¹³C NMR (δ-ppm): 15.94 (CH₃), 20.75 (CH₃), 20.97 (CH₃), 93.41, 100.49, 120.40, 125.03, 125.80, 128.96, 129.83, 135.64, 136.22, 138.01, 146.37, 160.49, 162.41 (ArC).

3-Bromomethyl-5-(5-hydroxy-3-methyl-1-phenyl-1H-pyrazol-4-yl)-7-methyl[1,2,4]triazolo[3,4-a]pyrimidine 21

A solution of the hydrazino derivative **18** (2.9 g, 10 mmol) in ethanol (20 mL) was refluxed with ethyl bromoacetate (0.167 g, 10 mmol) for 2 h. The reaction mixture was then concentrated to yield a white solid which was filtered, washed with ethanol, and recrystallized from ethanol. Physicochemical and analytical data are recorded in Table 4.

IR (cm⁻¹): 3356 (OH). ¹H NMR (δ-ppm): 2.37 (s, 3H, CH₃), 2.44 (s, 3H, CH₃), 4.76 (s, 2H, CH₂), 7.18–7.82 (m, 6H, ArH + H-6), 14.43 (s, 1H, exchangeable OH). ¹³C NMR (δ-ppm): 15.62 (CH₃), 22.47 (CH₃), 30.79 (CH₂), 96.82, 100.53, 120.99, 121.02, 126.99, 129.10, 129.15, 137.24, 147.12, 158.70, 163.56, 166.96 (ArC).

Ethyl 5-(5-hydroxy-3-methyl-1-phenyl-1H-pyrazol-4-yl)-7-methyl[1,2,4]triazolo[3,4-a]pyrimidine-3-carboxylate 22

A mixture of **18** (2.9 g, 10 mmol) and an excess of diethyl oxalate (7.3 g, 50 mmol) was refluxed for 3 h. The reaction was allowed to attain room temperature and the separated solid was collected by filtration and recrystallized from DMF. Physicochemical and analytical data are recorded in Table 4.

IR (cm⁻¹): 1702 (CO), 3356 (OH). ¹H NMR (δ-ppm): 1.35 (t, J = 8 Hz, 3H, CH₃), 2.39 (s, 3H, CH₃), 2.79 (s, 3H, CH₃), 4.30 (q, J = 8 Hz, 2H, CH₂), 7.42–7.55 (m, 6H, ArH + H-5), 15.13 (s, 1H, exchangeable OH). ¹³C NMR (δ-ppm): 8.6 (CH₃), 13.5 (CH₃), 21.2 (CH₃), 59.2 (CH₂), 107.8, 118.7, 119.63, 126.2, 129.0, 129.2, 139.6, 151.8, 152.2, 152.4, 164.2, 166.4, 167.3 (ArC), 167.3 (CO).

6-(5-Hydroxy-3-methyl-1-phenyl-1H-pyrazol-4-yl)-8-methyl-2H-pyrimido-[2,1-c][1,2,4]triazin-3,4-dione 23

A mixture of **18** (2.9 g, 10 mmol), sodium acetate (1.0 g), and diethyl oxalate (1.6 g, 11 mmol) in ethanol (30 mL) was refluxed for 8 h. The reaction mixture was poured into ice cold water and the precipitated solid product was filtered, washed with water, recrystallized from DMF. Physicochemical and analytical data are recorded in Table 4.

IR (cm⁻¹): 1662, 1667 (2 CO), 3356 (OH), 3386 (NH). ¹H NMR (δ-ppm): 2.12 (CH₃), 2.48 (CH₃), 7.10–7.87 (m, 7H, ArH +

pyrimidine H-5 + NH), 14.85 (s, 1H, exchangeable OH). ¹³C NMR (δ-ppm): 15.97 (CH₃), 20.78 (CH₃), 93.44, 100.51, 120.43, 125.06, 125.83, 128.99, 129.86, 135.66, 136.25, 138.03, 146.40 (ArC), 162.51 (CO), 167.78 (CO).

General procedure for the synthesis of 6-(5-hydroxy-3-methyl-1-phenyl-1H-pyrazol-4-yl)-8-methyl-3-substituted-2H-pyrimido-[2,1-c][1,2,4]triazines 24 and 25

A solution of the hydrazino derivative **18** (2.9 g, 10 mmol) in glacial acetic acid (15 mL) was refluxed with the appropriate β-bromoketone (10 mmol) for 2 h. After being cooled to room temperature, the mixture was poured onto crushed ice and the separated solid was filtered, washed with water, and recrystallized from DMF. Physicochemical and analytical data are recorded in Table 4.

IR (cm⁻¹) of compounds **24** and **25**: 3287–3298 (OH), 3358–3373 (NH). ¹H NMR (δ-ppm) of compound **24**: 2.18 (CH₃), 2.39 (CH₃), 2.52 (CH₃), 5.75 (s, 1H, C₄-H), 6.87–7.35 (m, 7H, ArH + NH + H-7), 15.62 (s, 1H, exchangeable OH). ¹³C NMR (δ-ppm) of compound **24**: 17.98 (CH₃), 20.04 (CH₃), 21.3 (CH₃), 89.56, 98.76, 109.18, 118.78, 123.65, 126.20, 129.07, 129.14, 139.67, 146.32, 153.84, 155.82, 164.65 (ArC). ¹H NMR (δ-ppm) of compound **25**: 2.02 (CH₃), 2.39 (CH₃), 6.69–7.52 (m, 12H, ArH + NH + H-7), 15.25 (s, 1H, exchangeable OH). ¹³C NMR (δ-ppm) of compound **25**: 19.97 (CH₃), 22.47 (CH₃), 93.52, 96.45, 107.43, 108.53, 114.55, 118.09, 121.23, 121.51, 124.91, 126.37, 128.64, 137.06, 140.50, 145.39, 146.61, 163.27, 163.79 (ArC).

General procedure for the synthesis of 3,6-dimethyl-1-substituted pyrano[2,3-c]pyrazole-4(1H)-ones 26 and 27

To a solution of the appropriate pyrazole diketone **4** or **5** (10 mmol) in acetic acid (20 mL) was added dropwise concentrated sulfuric acid (1 mL). The mixture was allowed to stand at room temperature for 2 h, then poured carefully onto crushed ice. The formed precipitate was filtered, washed several times with cold water, dried, and recrystallized from ethanol/DMF (4:1). Physicochemical and analytical data are recorded in Table 4.

IR (cm⁻¹) of compounds **26** and **27**: 1660–1664 (CO), 1152, 1375 (SO₂N for compound **17**). ¹H NMR (δ-ppm) of compound **26**: 2.10 (s, 3H, CH₃), 2.44 (s, 3H, CH₃), 5.41 (s, 1H, pyrane C₃-H), 7.04–7.32 (m, 5H, ArH). ¹³C NMR (δ-ppm) of compound **26**: 14.89 (CH₃), 21.22 (CH₃), 98.24, 112.54, 118.98, 126.02, 129.21, 129.43, 139.56, 150.43, 164.73 (ArC), 185.89 (CO). ¹H NMR (δ-ppm) for compound **27**: 2.04 (s, 3H, CH₃), 2.47 (s, 3H, CH₃), 5.32 (s, 1H, pyrane C₃-H), 6.89–7.43 (m, 6H, ArH + NH₂). ¹³C NMR (δ-ppm) for compound **27**: 15.94 (CH₃), 20.66 (CH₃), 93.10, 114.40, 120.37, 126.83, 128.96, 131.06, 138.03, 146.36, 162.96 (ArC), 183.66 (CO).

5-Chloro-3,6-dimethyl-1-phenylpyrano[2,3-c]pyrazole-4(1H)-one 29

To a solution of the pyrazole **4** (2.5 g, 10 mmol) in dry methylene chloride (20 mL) was added dropwise sulfuric chloride (1.35 g, 10 mmol). The reaction mixture was allowed to stand at room temperature for 2 h, then poured into a

stirred solution of 10% aqueous K_2CO_3 (50 mL) over 5 min. The aqueous layer was acidified with 10% hydrochloric acid and extracted with chloroform (3×10 mL). The combined organic extracts were washed with water and dried over anhydrous sodium sulfate, then the solvent was removed under reduced pressure. The left crude compound **28** was directly treated with concentrated sulfuric acid (10 mL) and the mixture was left at room temperature for 4 h then poured carefully onto crushed ice. The product formed was extracted with chloroform (3×10 mL), the chloroformic extract was washed with 5% aqueous K_2CO_3 solution, dried over anhydrous sodium sulfate, and evaporated *in vacuo* to dryness to give the product **29**, which was recrystallized from acetonitrile. Physicochemical and analytical data are recorded in Table 4.

IR (cm^{-1}): 1665 (CO). 1H NMR (δ -ppm): 2.20 (s, 3H, CH_3), 2.49 (s, 3H, CH_3), 7.21–7.67 (m, 5H, ArH). ^{13}C NMR (δ -ppm): 11.32 (CH_3), 18.59 (CH_3), 97.96, 101.51, 119.68, 125.04, 128.97, 137.74, 139.76, 141.75, 145.90, 164.82 (ArC), 186.56 (CO).

General procedure for the synthesis of 5-trifluoroacetyl-3,6-dimethyl-1-substituted-pyrano[2,3-c]pyrazole-4(1H)-ones **32** and **33**

A solution of the appropriate pyrazole **4** or **5** (10 mmol) in THF (20 mL) was refluxed with trifluoroacetic anhydride for 4 h. Removal of the solvent *in vacuo* afforded compounds **30** and **31** in crude state. Working up of the reaction mixture was carried out as described under compound **29**. The products were recrystallized from DMF. Physicochemical and analytical data are recorded in Table 4.

IR (cm^{-1}) of compounds **32** and **33**: 1662–1668, 1669–1672 (2 CO), 1142, 1369 (SO_2N for compound **33**). 1H NMR (δ -ppm) of compound **32**: 2.09 (s, 3H, CH_3), 2.42 (s, 3H, CH_3), 7.06–7.35 (m, 5H, ArH). ^{13}C NMR (δ -ppm) of compound **32**: 16.80 (CH_3), 20.77 (CH_3), 128.70 (CF_3), 93.01, 100.38, 114.08, 120.12, 125.83, 126.58, 126.83, 131.48, 138.49, 146.50, 158.60, 160.62, 162.16 (ArC), 183.66 (CO), 196.60 ($COCF_3$). 1H NMR (δ -ppm) of compound **33**: 2.07 (s, 3H, CH_3), 2.48 (s, 3H, CH_3), 6.73–7.99 (m, 6H, ArH + NH_2). ^{13}C NMR (δ -ppm) of compound **33**: 15.46 (CH_3), 20.84 (CH_3), 128.98 (CF_3), 108.38, 112.86, 115.41, 119.62, 129.10, 129.32, 144.32, 152.42, 164.25 (ArC), 185.23 (CO), 196.20 ($COCF_3$).

Biological evaluation

Carrageenan-induced paw edema bioassay

All the synthesized 27 compounds (**4–27**, **29**, **32**, and **33**) were evaluated for their *in vivo* systemic anti-inflammatory activity using the carrageenan-induced paw edema bioassay in rats as a model of acute inflammation [35]. Male albino rats weighing 120–150 g were used throughout the work. They were kept in the animal house under standard conditions of light and temperature with free access to food and water. The animals were randomly divided into groups of five rats each. The paw edema was induced by subplantar injection of 50 μ L of 2% carrageenan solution in saline (0.9%). Indomethacin, celecoxib (reference anti-inflammatory drugs), and the test compounds were dissolved in DMSO and were injected subcutaneously in a dose of 10 μ mol/kg body weight, 1 h

prior to carrageenan injection. Control group was injected with DMSO only. The volume of paw edema (mL) was determined by means of plethysmometer immediately after injection of carrageenan and 4 h later. The increase in paw volume between time 0 h and 4 h was measured and the percentage protection against inflammation was calculated according to the following equation:

$$\text{Protection against inflammation (\%)} = (V_c - V_d) / V_c \times 100$$

where V_c is the increase in paw volume in the absence of test compound (control) and V_d is the increase in paw volume after injection of the test compound. Data were expressed as the mean \pm SE. Statistical differences of control and test groups were carried out using the analysis of variance (ANOVA) followed by "Student–Newman–Keuls Multiple Comparison Test". They were performed using computer package of the Statistical Analysis System (SAS, 1987), SAS Incorporation Institute. The difference in results was considered significant when $P < 0.05$. The obtained data are recorded in Table 1. Additionally, the ED_{50} values for the most potent derivatives **5**, **10**, **17**, **19**, and **27** were determined using three different doses, and the paw thickness of each rat was measured after 4 h of carrageenan injection according to the literature procedure [36].

In vitro COX-1 and COX-2 inhibitory assay

All the developed 27 target compounds (**4–27**, **29**, **32**, and **33**) were evaluated for their ability to inhibit COX-1 and COX-2 isozymes employing an ovine COX-1/COX-2 inhibitor screening assay kit (Catalog No. 760111, Cayman Chemicals, Inc., Ann Arbor, MI, USA) according to the manufacturer's instructions and literature procedure [37, 38]. The method relied on the peroxidase component of COX which is assayed colorimetrically by monitoring the appearance of oxidized *N,N,N',N'*-tetramethyl-1,4-phenylenediamine (TMPD), that is generated during the reduction of PGG₂ to PGH₂, at 590 nm. The efficiencies of the investigated compounds were measured as the concentration causing 50% enzyme inhibition (IC_{50} ; μ M), the selectivity index (SI value) was calculated as IC_{50} (COX-1)/ IC_{50} (COX-2). Indomethacin and celecoxib were used as reference standard in the study.

Ulcerogenic effects

Compounds **5**, **10**, **17**, **19**, and **27** were evaluated for their ulcerogenic potential in rats according to a reported procedure [39]. Indomethacin and celecoxib were used as reference standard anti-inflammatory drugs. Male albino rats (100–120 g) were fasted for 12 h prior to the administration of the compounds. Water was given *ad libitum*. The animals were divided into groups, each of five animals. Control group received 1% gum acacia orally. Other groups received indomethacin, celecoxib or the test compounds orally in two equal doses at 0 and 12 h for three successive days at a dose of 30 μ mol/kg per day. Animals were sacrificed under ether anesthesia 6 h after the last dose and the stomach was removed. An opening at the greater curvature was made and

the stomach was cleaned by washing with cooled saline and inspected with a 3× magnifying lens for any evidence of hyperemia, hemorrhage, definite hemorrhagic erosion, or ulcer. An arbitrary scale was used to calculate the ulcer index which indicates the severity of the stomach lesions, and the percentage of ulceration for each group was calculated and recorded in Table 1 as follows:

$$\% \text{Ulceration} = \frac{\text{Number of animals bearing ulcer in a group}}{\text{Total number of animals in the same group}} \times 100$$

Acute toxicity

Compounds **5**, **10**, **17**, **19**, and **27** were investigated for their oral acute toxicity in male mice according to the method described by Litchfield and Wilcoxon [40]. The animals (20 g each) were divided into groups (each of six mice), and the tested compounds were given orally, suspended in 1% gum acacia, in doses of 1, 10, 100, 200, 250, 500 mg/kg, respectively. Twenty-four hours later, the percentage mortality in each group and for each compound was recorded and the acute lethal doses (ALD₅₀) values were calculated.

In addition, the same compounds were tested for their parenteral acute toxicity in groups each of six of mice (20 g each). The compounds or their vehicle, propylene glycol (control), were given by intraperitoneal injection in doses of 5, 10, 20, 40, 80 mg/kg and the percentage survival was followed up to 7 days [41].

This project was funded by (SABIC) and the Deanship of Scientific Research (DSR) at King Abdulaziz University, Jeddah, under grant no. S-17-416-37. The authors, therefore, acknowledge with thanks SABIC and DSR for technical and financial support. The authors are also deeply thankful to the authorities of City of Science and Technology, Alexandria, Egypt, for their efforts and assistance in performing the biological assays.

The authors have declared no conflict of interest.

References

- [1] V. Alagarsamy, V. Raja Solomon, R. Meena, K. V. Ramaseshu, K. Thirumurugan, S. Murugesan, *Med. Chem.* **2007**, *3*, 67–73.
- [2] I. K. Khanna, Y. Yu, R. M. Huff, R. M. Weier, X. Xu, F. J. Koszyk, P. W. Collins, J. N. Cogburn, P. C. Isakson, C. M. Koboldt, J. L. Masferrer, W. E. Perkins, K. Seibert, A. W. Veenhuizen, J. Yuan, D-C. Yang, Y. Y. Zhang, *J. Med. Chem.* **2000**, *43*, 3168–3185.
- [3] S. F. Long, in *Comprehensive Pharmacy Review* (Eds.: L. Shargel, A. H. Mutnick, P. F. Souney, L. N. Swanson), Lippincott Williams and Wilkins, Philadelphia **2001**, pp. 289–291.
- [4] Y. Song, D. T. Connor, R. Doubleday, R. J. Sorenson, A. D. Sercel, P. C. Unangst, B. D. Roth, R. B. Gilbertsen, K. Chan, D. J. Schrier, A. Guglietta, D. A. Bornemeier, R. D. Dyer, *J. Med. Chem.* **1999**, *42*, 1151–1160.
- [5] C. Puig, M. I. Crespo, N. Godessart, J. Feixas, J. Ibarzo, J-M. Jimenez, L. Soca, I. Cardelus, A. Heredia, M. Miralpeix, J. Puig, J. Beleta, J. M. Huerta, M. Lopez, V. Segarra, H. Ryder, J. M. Palacios, *J. Med. Chem.* **2000**, *43*, 214–223.
- [6] A. S. Kalgutkar, A. B. Marnett, B. C. Crews, R. P. Rimmel, L. J. Marnett, *J. Med. Chem.* **2000**, *43*, 2860–2870.
- [7] M. Inagaki, T. Tsuru, H. Jyoyama, T. Ono, K. Yamada, K. Kobayashi, Y. Hori, A. Arimura, K. Yasui, K. Ohno, S. Kakudo, K. Koizumi, R. Suzuki, M. Kato, S. Kawai, S. Matsumoto, *J. Med. Chem.* **2000**, *43*, 2040–2048.
- [8] B. Hinz, K. Brune, *J. Pharmacol. Exp. Ther.* **2002**, *300*, 367–375.
- [9] A. J. Scheen, *Rev. Med. Liege* **2004**, *59*, 565–569.
- [10] A. A. Bekhit, H. T. Y. Fahmy, *Arch. Pharm. Pharm. Med. Chem.* **2003**, *2*, 111–118.
- [11] E. Banoglu, Ç. Akoglu, S. Ünlü, E. Küpeli, E. Yesilada, M. F. Sahin, *Arch. Pharm. Pharm. Med. Chem.* **2004**, *337*, 7–14.
- [12] A. A. Bekhit, H. M. A. Ashour, A. Guemei, *Arch. Pharm. Chem. Life Sci.* **2005**, *338*, 167–174.
- [13] O. Rosati, M. Curini, M. C. Marcotullio, A. Macchiarulo, M. Perfumi, L. Mattioli, F. Rismondo, G. Cravotto, *Bioorg. Med. Chem.* **2007**, *15*, 3463–3473.
- [14] G. Szabó, J. Fischer, A. Kis-Varga, K. Gyires, *J. Med. Chem.* **2008**, *51*, 142–147.
- [15] R. Fioravanti, A. Bolasco, F. Manna, F. Rossi, F. Orallo, F. Ortuso, S. Alcaro, R. Cirill, *Eur. J. Med. Chem.* **2010**, *45*, 6135–6138.
- [16] M.A.-A. El-Sayed, N. I. Abdel-Aziz, A.A.-M. Abdel-Aziz, A. S. El-Azab, Y. A. Asiri, K. E. H. ElTahir, *Bioorg. Med. Chem.* **2011**, *19*, 3416–3424.
- [17] K. R. A. Abdellatif, W. A. A. Fadaly, A. A. Azouz, *Arch. Pharm. Chem. Life Sci.* **2016**, *349*, 801–807.
- [18] A. Palomer, F. Cabre, J. Pascual, J. Campos, M. A. Trujillo, A. Entrena, M. A. Callo, L. Garcia, D. Mauleon, A. Espinosa, *J. Med. Chem.* **2002**, *45*, 1402–1411.
- [19] S. A. F. Rostom, M. A. Shalaby, M. A. El-Demellawy, *Eur. J. Med. Chem.* **2003**, *38*, 959–974.
- [20] S. A. F. Rostom, *Bioorg. Med. Chem.* **2006**, *14*, 6475–6485.
- [21] H. M. Faidallah, M. S. Al-Saadi, S. A. F. Rostom, H. T. Y. Fahmy, *Med. Chem. Res.* **2007**, *16*, 300–318.
- [22] M. S. Al-Saadi, S. A. F. Rostom, H. M. Faidallah, *Arch. Pharm. Chem. Life Sci.* **2008**, *341*, 181–190.
- [23] S. A. F. Rostom, *Bioorg. Med. Chem.* **2010**, *18*, 2767–2776.
- [24] S. A. F. Rostom, H. A. Abd El Razik, M. H. Badr, H. M. A. Ashour, *Arch. Pharm. Chem. Life Sci.* **2011**, *344*, 572–587.
- [25] H. M. Faidallah, K. A. Khan, S. A. F. Rostom, A. M. Asiri, *J. Enz. Inhib. Med. Chem.* **2013**, *28*, 495–508.
- [26] H. M. A. Ragab, A. A. Bekhit, S. A. F. Rostom, A. E. A. Bekhit, *Curr. Top. Med. Chem.* **2016**, *16*, 3569–3581.
- [27] A. M. Farghaly, F. S. G. Soliman, M. M. El-Semary, S. A. F. Rostom, *Pharmazie* **2001**, *56*, 28–32.

- [28] A. M. Asiri, H. M. Faidallah, H. A. Albar, M. S. Makki, E. M. Sharshira, *Phosphorous Sulfur Silicon* **2002**, *177*, 685–693.
- [29] A. M. Asiri, H. M. Faidallah, H. A. Albar, E. M. Sharshira, *Heterocycl. Comm.* **2003**, 483–488.
- [30] A. A. Bekhit, H. T. Y. Fahmy, S. A. F. Rostom, A. M. Baraka, *Eur. J. Med. Chem.* **2003**, *38*, 27–36.
- [31] S. A. F. Rostom, I. M. El-Ashmawy, H. A. Abd El Razik, M. H. Badr, H. M. A. Ashour, *Bioorg. Med. Chem.* **2009**, *17*, 882–895.
- [32] A. A. Bekhit, H. T. Y. Fahmy, S. A. F. Rostom, A. E. A. Bekhit, *Eur. J. Med. Chem.* **2010**, *45*, 6027–6038.
- [33] H. M. Faidallah, S. A. F. Rostom, K. A. Khan, *Arch. Pharm. Res.* **2015**, *38*, 203–215.
- [34] H. M. Faidallah, M. S. Makki, S. A. Basaif, S. B. Al-Masaydi., *AFINIDAD LV* **1998**, *475*, 202–206.
- [35] M. Di Rosa, D. A. Willoughby, *J. Pharm. Pharmacol.* **1971**, *23*, 297–298.
- [36] C. A. Winter, E. A. Risley, G. W. Nuss, *Proc. Soc. Exp. Biol. Med.* **1962**, *111*, 544–547.
- [37] R. J. Kulmacz, W. E. M. Lands, *Prostaglandins* **1983**, *25*, 531–540.
- [38] B. Roschek, R. C. Fink, D. Li, M. McMichael, C. M. Tower, R. D. Smith, R. S. Alberte, *J. Med. Food* **2009**, *12*, 615–625.
- [39] M. S. Abouzeit-Har, T. Verimer, J. P. Long, *Pharmazie* **1982**, *37*, 593–595.
- [40] J. T. Litchfield, F. Wilcoxon, *J. Pharmacol. Exp. Ther.* **1949**, *96*, 99–113.
- [41] A. A. Bekhit, T. Abdel-Azeim, *Bioorg. Med. Chem* **2004**, *12*, 1935–1945.
- [42] C. A. Lipinski, L. Lombardo, B. W. Dominy, P. J. Feeney, *Adv. Drug Deliv. Rev.* **2001**, *46*, 3–26.
- [43] D. F. Veber, S. R. Johnson, H. Y. Cheng, B. R. Smith, K. W. Ward, K. D. Kopple, *J. Med. Chem.* **2002**, *45*, 2615–2623.
- [44] Molinspiration Chemoinformatics. Brastislava, Slovak Republic. **2014**. <http://www.molinspiration.com/cgi-bin/properties>.
- [45] Y. Zhao, M. H. Abraham, J. Lee, A. Hersey, N. C. Luscombe, G. Beck, B. Sherborne, I. Cooper, *Pharm. Res.* **2002**, *19*, 1446–1457.
- [46] OSIRIS Property Explorer: version 2. **2014**. <http://www.organic-chemistry.org/prog/peo/>.
- [47] S. Gelin, B. Chantegrel, A. Nadi, *J. Org. Chem.* **1983**, *48*, 4078–4082.
- [48] N. Sellier, *J. Heterocycl. Chem.* **1999**, *36*, 1291–1294.
- [49] N. Benaamane, B. Nedjar-Kolli, Y. Bentarzi, L. Hammal, A. Geronikaki, P. Eleftheriou, A. Lagunin, *Bioorg. Med. Chem.* **2008**, *16*, 3059–3066.